THE GEOSYNCHRONOUS ORBITAL REGION AND REACHING IT FROM LOWER APOGEE ALTITUDES

D. K. Skoulidou and S. Lemmens

ESA/ESOC, Robert-Bosch-Str. 5, 64293 Darmstadt, Germany, Email: {despoina.skoulidou, stijn.lemmens}@esa.int

ABSTRACT

Recently, there were 127 rocket bodies found crossing the GEO protected region, where a significant number of them were placed in lower altitudes (sub-GEO region). The most recent guidelines of ESA have suggested possible space debris mitigation measures for launch vehicle stages, indicating to lower the apogee below the operational (e.g. lower than 550 km from r_{GEO}). This becomes relevant with the advent of new direct to GEO missions. Since the late 90's, the IADC guidelines, for the disposal of a spacecraft placed in GEO, suggest the disposal in near-circular graveyard orbits above the GEO protected region, where the altitude of perigee is beyond the 235km plus a factor accounting for the solar radiation pressure perturbations. The aim of this study is to investigate the sub-GEO region and if an upper apogee difference limit exist, where the orbits are compliant with the current guidelines, for a time span of 100yr at least, and if it is still feasible to reach the GEO protected region.

Keywords: geosynchronous; dynamics; artificial satellites; space debris.

1. INTRODUCTION

The second most populated region after the Low Earth Orbital region (LEO) is around the geosynchronous altitude. Artificial satellites are placed around the $1:1$ spin orbital resonance, where the orbital period of the satellite is equal to the spin period of Earth, of about one sidereal day. Geosynchronous Earth Orbits (GEO) have a semi-major axis of about $r_{GEO} = 42165$ km.

Satellites placed in the GEO region are used for telecommunications, air traffic management etc., and hence, need to be disposed form the operational region to clear the longitude slots for future missions. Since the late 90's, has been defined the GEO protected region[1], and satellites are disposed outside that region at post-mission stage. The IADC guidelines, for the disposal of a spacecraft placed in GEO, suggest the disposal in near-circular graveyard orbits above the GEO protected region (super-GEO region), where the altitude of perigee is of the form

$$\Delta H = 235 + 1000 \cdot C_r \frac{A}{m}, \tag{1}$$

where C_r and A/m are the reflectivity coefficient and the aspect area to dry mass ratio $\left(m^2 kg^{-1}\right)$, respectively, and an eccentricity $e \leq 0.003$ [8].

Numerous dynamical studies have been performed for the stability of the disposal orbits in the super-GEO region (e.g., [3], [4], [9], [1]). Equation 1 is valid without constrains for disposal orbits with low eccentricity values ($e < 0.005$), as the variations in such low e is mainly driven by perturbations due to the Solar Radiation Pressure (SRP), as they are prevailing over the luni-solar perturbations. Larger sensitivities to the values of initial perigee and eccentricity were found, and minor ones to the values of the right ascension of the ascending node (Ω), argument of perigee (ω), and epoch. A smaller altitude increase can be achieved, in terms of compliancy of the graveyard orbit for at least of 100yr time-interval, with a choice of a Sun-pointing perigee. This solution ensures that the eccentricity will remain constant and the influence of the SRP will have no more effect on the altitude of perigee, but also implies that the disposal should be performed at a suitable epoch. For larger eccentricities (even up to 0.3), optimal solutions, in terms of compliancy of the graveyard orbit for at least of 100yr time-interval, can be achieved with a suitable combination of the perigee pointing, varying with a period of 1yr, and the value of Ω_M (i.e., Ω of the Moon), varying with a period of 18.6yr.

Recently, there were 127 rocket bodies found crossing the GEO protected region [5], where a significant number of them were placed in lower altitudes (sub-GEO region). The most recent guidelines of ESA [6] have suggested possible space debris mitigation measures for launch vehicle stages, indicating to lower the apogee below the operational (e.g. lower than 550 km from r_{GEO}). This becomes relevant with the advent of new direct to GEO missions.

The aim of this study is to investigate the sub-GEO region

[1] The GEO protected region is defined at the semi-major axis range, $a = r_{GEO} \pm 200$ km, and a latitude sector from 15° South to 15° North [8][6]

Table 1: Grids of initial conditions for the sub-GEO study.

$\mathbf{a}$ $(\mathbf{km})$	$40357 - 41944$
$\mathbf{e}$	$0.0001 - 0.2$
$\mathbf{i}$ $(^\circ)$	$0.5 - 18$
Ω $(^\circ)$	$\{0, 60, 120, 180, 240, 300\}$
$(\Omega + \omega - \lambda_s)$ $(^\circ)$	$\{0, 60, 120, 180, 240, 300\}$

and if an upper apogee deference limit[2], $(r_{GEO} - Q)$, exist, where the orbits are compliant with the current guidelines, for a time span of 100yr at least, and if it is still feasible to reach the GEO protected region from these orbits with a low delta V penalty. In section 2, we describe the dynamical model used and the choice of the nitial conditions. A subset of our results is presented in section 3, followed by the conclusions in section 4.

2. PROBLEM FORMULATION

2.1. Model

A satellite orbiting around the Earth is affected mainly by the following perturbations: the Earth's oblateness, the higher harmonics of the Earth's geopotential, the lunar and solar gravitational fields, the direct solar radiation pressure and atmospheric drag. The latter particularly affects low-altitude orbits in the LEO region.

In our study, we wish to understand the long-term dynamical behaviour of satellite orbits, focusing on the GEO region. For that purpose, we use the orbit propagator FOCUS-2 included in OSCAR of the ESA DRAMA suite, which performs the integration of the singly averaged Gauss variational equations for Keplerian elements. The target orbit to introduce to OSCAR is defined by singly averaged Keplerian elements (i.e., the input should be in terms of mean elements, and, hence, all results presented are in terms of mean elements)[2].

The default dynamical model taken into account in the OSCAR propagator is the geopotential up to 6 degree and order $(J_{6,6})$ using Goddard Earth Model GEMT1 , lunisolar perturbations, Solar Radiation Pressure (SRP) defined by the cannonball model + a cylindrical shadow (no Earth flattening for shadow), acceleration due to atmospheric drag from NRLMSISE-00 model, and solar and geomagnetic activity compliant with ISO 27852:2016 / ECSS-E-ST-10-04C: the latest prediction's-method.

One of the options in OSCAR is to check if the examined object is crossing the protected GEO region or not during the propagation. Since, the main goal of this study is to investigate the compliancy in the sub-GEO region, this option is activated by giving the answer "yes/no crossing" without performing a deeper analysis on the time spending within the GEO protected region.

2.2. Initial Conditions

Our goal is to obtain a view of the long-term dynamics of the sub-GEO region. For that purpose, we covered a wide range in orbital elements space and propagated the initial conditions over a long timescale (100 years). The summary of the initial conditions is given in Table 1. The grid of initial conditions covers apogee values, Q, from $r_{GEO} - 1000\ km$ and up to $r_{GEO} - 200\ km$. The argument of perigee, ω, is computed by combination of Ω and angle, $\phi = \Omega + \omega - \lambda_s$, where λ_s is the ecliptic latitude of the Sun for specific epoch. The ϕ angle corresponds to the angle between the apsidal line[3] and the direction of the Sun. When $\phi = 0$ or 180° the perigee or the apogee is Sun-pointing, respectively. The initial mean anomaly was set equal to zero, $M = 0$, for all cases.

In the first part of this study (see 3.1), the A/m is set fixed and equal to $0.0128\ m^2/kg$, which is the mean value of the current payload population placed around the GEO region, as exported form the ESA's DISCOS[10] , and the $C_r = 1.3$. In the second part of this study (see 3.2), a range of values of the $A/m \in [0.02, 0.2]\ m^2/kg$ and 3 values of $C_r = \{1, 1.3, 2\}$ are examined. The drag coefficient, C_d, was set equal to 2.2 for all cases and has no real influence near GEO.

The study was performed for one selected initial epoch, 2022/06/09 12:00:00 UTC, where $\lambda_s = 77.66^\circ$ [4]. In studies for the stability of the disposal orbits in the super-GEO region (e.g., see [1]), the chosen epochs were usually the summer and winter solstice, where $\lambda_s = 90^\circ$ and $\lambda_s = 120^\circ$, and hence, the examined $(\Omega + \omega) = 90^\circ$ and $(\Omega + \omega) = 120^\circ$ corresponded to a Sun-pointing perigee, respectively. That was implying that the disposal of the satellite should be performed around these two dates of the year, as also the proper position of the satellite to secure the Sun-pointing geometry. In this study, we are following a different approach. We would expect that a Sun-pointing apsidal line to correspond to the minimum $(r_{GEO} - Q)$ that could be compliant, and this could be achieved at any date within a year, in combination with the suitable choice of initial conditions, which might not suite to the summer or the winter solstice.

[2]Since we examined the sub-GEO region, the apogee values are always lower than the Geosynchronous radius, r_{GEO}. Hence, we define the (positive) quantity $(r_{GEO} - Q)$ as the apogee difference. r_{GEO} and Q are w.r.t. the centre of the Earth. Altitude is defined as the distance from Earth's surface.

[3]The apsidal line connects the perigee and the apogee

[4]The λ_s value was computed using the equations provided in sec. 5.1.1 of [12]

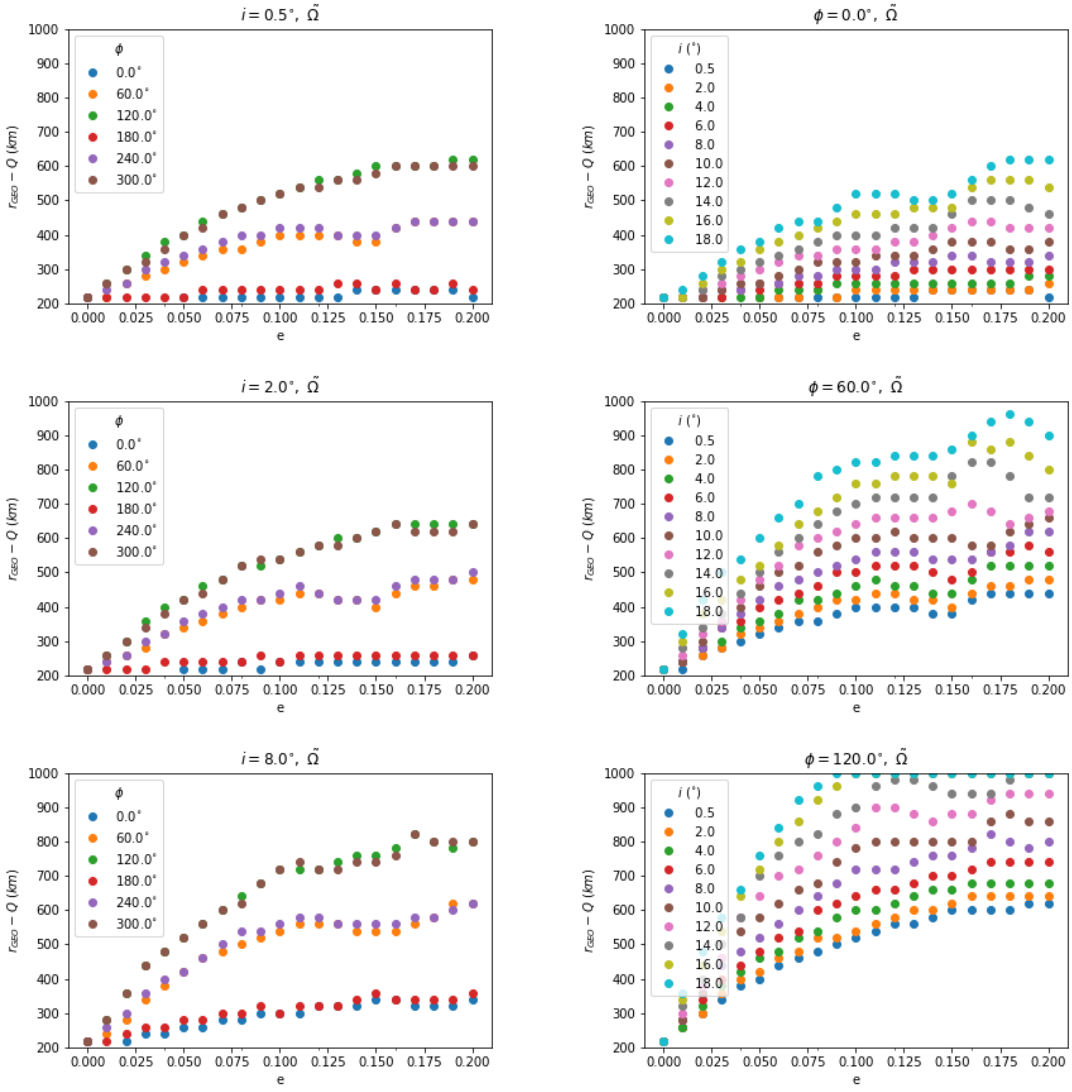

Figure 1: Plot of the maximum initial apogee difference,$(r_{GEO} - Q)$, that is compliant w.r.t. initial eccentricity, e.
(left) for three different values of initial inclination, i, $0.5°$ (top), $2°$ (middle), and $8°$ (bottom). The colours denote the initial ϕ angle.
(right) for three different ϕ angles, 0 (top), $60°$ (middle), and $120°$ (bottom). The colours denote the initial inclination, i

3. RESULTS

3.1. Fixed A/m

For the simulations with fixed $A/m = 0.0128\ m^2/kg$, for specific values of i, ϕ, and e, the maximum apogee difference that is compliant was found, from all the examined Ω values. Fig.1(left) shows the maximum $(r_{GEO} - Q)$ that is compliant for every initial e and for initial $i = 0.5°$ (top), $2°$ (middle), and $8°$ (bottom). The colours denote the initial ϕ angle. Fig.1(right) shows the maximum $(r_{GEO} - Q)$ that is compliant for every initial e and for initial $\phi = 0$ (top), $60°$ (middle), and $120°$ (bottom). The colours denote the initial i.

According to the results, when $\phi = 0$ or $180°$, which denotes that the apsidal line is Sun-pointing, the minimum compliant $(r_{GEO} - Q)$ is achieved, which is up to $\sim 250\ km$ for all the low-inclined orbits $(i < 4°)$. The results are consistent with those exported from similar studies performed in the super-GEO region (e.g., [3, 1]). The compliant apogee difference is up to $\sim 500-600\ km$ as the inclination increases and for $e = 0.1 - 0.2$. The compliant $(r_{GEO} - Q)$ becomes higher when $\phi = \{60°, 240°\}$ or $\{120°, 300°\}$, and for non-circular and inclined orbits, as the third-body perturbations leading over SRP perturbations.

3.2. Modified A/m

Table 2: Mean and standard deviation (std) values of b_r and c for each examined e and for $\phi = 0, 120°$.

ϕ	e	$\tilde{b}_r$ $(km \cdot kg \cdot m^{-2})$	std of b_r	$\tilde{c}$ (km)	std of c
0	0.0001	529.47	7.00	211.41	1.33
	0.001	428.26	19.01	201.36	2.18
	0.01	369.70	7.93	192.56	1.99
120°	0.0001	530.35	4.25	217.81	0.73
	0.001	531.0	4.27	220.15	0.97
	0.01	517.12	10.28	253.19	4.32

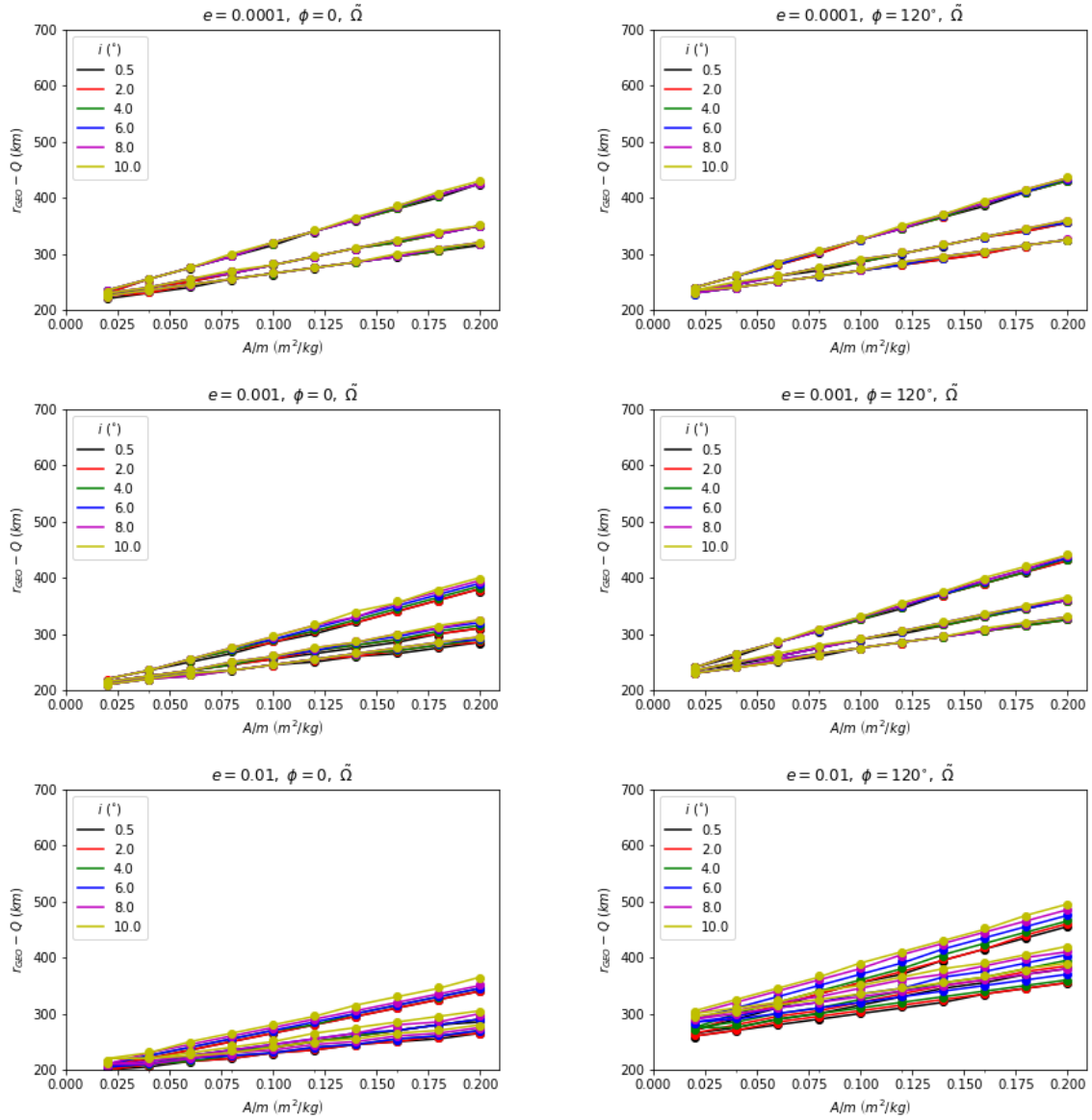

Figure 2: Plot of the $A/m - (r_{GEO} - Q)$ values (plotted points). $(r_{GEO} - Q)$ is the maximum initial apogee difference that is compliant w.r.t. Ω values, for each of A/m and C_r values. Different colour is for different i value, but for all the C_r values. Rows are for three e values, 10^{-4} (top), 10^{-3} (middle), 10^{-2} (bottom), and columns for two ϕ angle values, 0 (left), and 120° (right). Solid lines represent eq.2 for each i and C_r values.

The main goal of this part of the study was to investigate if the apogee difference could be a function of $C_r A/m$ and if a similar equation of 1 could be retrieved. For that purpose, we examine a grid of initial conditions where $Q \in [r_{GEO} - 700, r_{GEO} - 200]$ km, $e = 10^{-4}, 10^{-3}, 10^{-2}$ (i.e., 3 values which differ in order of magnitude), and in a wide range of $i \in [0.5°, 10°]$. The rest of the orbital elements and physical properties of

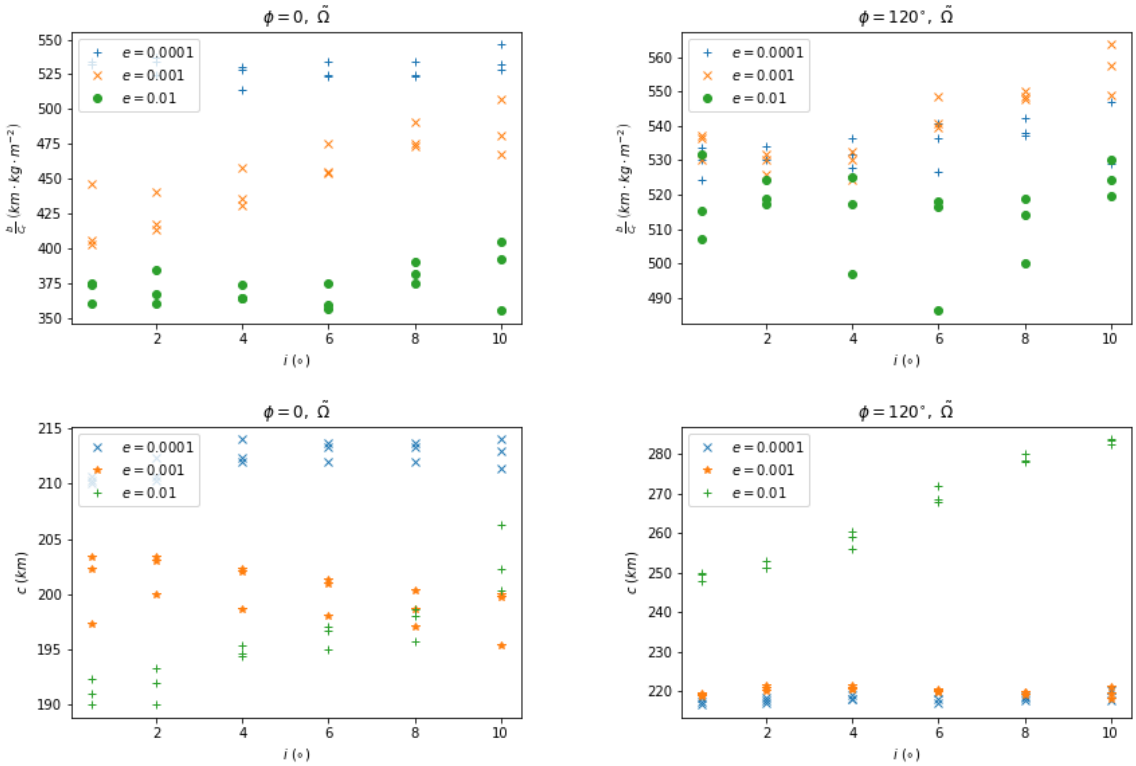

Figure 3: Plot of the $i - b_r$ (top) and $i - c$ (bottom), where $b_r = \frac{b}{C_r}\ \left(km \cdot kg \cdot m^{-2}\right)$, and b and c is the slope and the constant term of eq.2, respectively. The results are for all the examined e (different colors), C_r, and Ω values, and for two ϕ angle values, 0 (left), and 120° (right).

the objects are set as defined in sec.2.2.

Figure 2 shows the $A/m - (r_{GEO} - Q)$ values (plotted points). $(r_{GEO} - Q)$ is the maximum initial apogee difference that is compliant w.r.t. Ω values, for each of A/m and C_r values. Different colour is for different i value, but for all the C_r values. Plots in rows are for different e, 10^{-4} (top), 10^{-3} (middle), 10^{-2} (bottom), and in columns for two ϕ angle values, 0 (left), and 120° (right). Then we used the least square fit method (lsf) for the pairs $\{A/m, (r_{GEO} - Q)\}$. The form of the equation is:

$$(r_{GEO} - Q) = b \cdot \frac{A}{m} + c, \tag{2}$$

where b is the slope (in $km \cdot kg \cdot m^{-2}$) and c is the constant term (in km). We also set the quantity $b_r = b/C_r$ (also in $km \cdot kg \cdot m^{-2}$) , and, hence, eq.2 takes the form:

$$(r_{GEO} - Q) = b_r \cdot C_r \cdot \frac{A}{m} + c. \tag{3}$$

The solid lines of Fig.2 represents equation 2 for all the examined i and C_r values.

Figure 3 shows $i - b_r$ (top) and $i - c$ (bottom), for $\phi = 0$ (left) and 120° (right). Colour is for the examined e values. According to the plots, b_r and c slightly increase as i increases and it seams are not affected with the increasing of the C_r value, but further investigation of this is out of scope of the current study. We would like to remind that eq.1, for the perigee altitude at the super-GEO region, is valid for near circular and non-inclined orbits. Hence, we computed the mean and the standart deviation (std) of b_r and c for $i \leq 4°$ and separately for each combination of e and ϕ values. The results are shown in Tab.2. When $\phi = 0$, where the apsidal line is Sun-pointing, b_r is significant decreasing as e is increasing, from $\sim$ 530 to $\sim$ 370 $km \cdot kg \cdot m^{-2}$, whereas, when $\phi = 120°$, $b_r \sim 530\ km \cdot kg \cdot m^{-2}$. The constant term, c, is around 220 km.

3.3. Feasible manoeuvres from the sub-GEO to the GEO protected region

In the previous sections, we examined which are the apogee difference limits that an object could be placed and be compliant for 100 yr of time-span in the sub-GEO region. However, the cost of the manoeuvre required for an object to be transferred from the sub-GEO to the GEO protected region should also be considered. For example, it should be secured, when the separation between the Payload and the Rocket body is to be held, that the Rocket body will stay in a position compliant for at least 100 yr, and the ΔV required for the Payload's transfer not be prohibitively high.

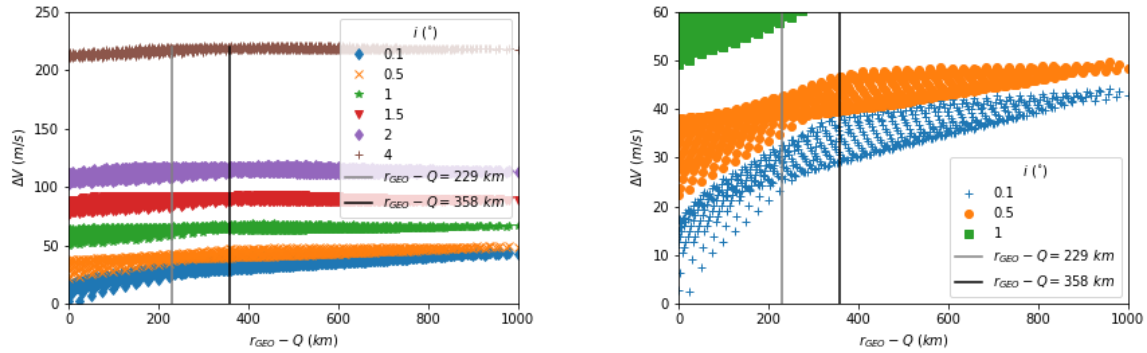

Figure 4: Plots show the ΔV required to reach a geosynchronous orbit from sub-GEO region with respect to the apogee difference $(r_{GEO} - Q)$. The colour denotes the inclination of the starting orbit, O_1. The vertical grey and black lines correspond to $(r_{GEO} - Q) = 530 \cdot C_r \frac{A}{m} + 220$, for $C_r = 1.3$ and $A/m = 0.0128\ m^2/kg$ and $A/m = 0.2\ m^2/kg$, respectively. The right plot is a zoom of the left plot for $\Delta V \leq 60\ m/s$.

For the computation of ΔV, the *Lambert problem* is used, which is known as the problem of defining an arc between two position vectors and the time of flight between them (see chapter 7 of [12] for details). The code used in this study has been implemented by ESA [5]. As starting orbit, (O_1), a grid in (a, e) was considered, where $a_1 \in [r_{GEO} - 1000, r_{GEO}]$ and $e_1 \in [0, 0.01]$, and for specific inclination values $i_1 = \{0.1°, 0.5°, 1°, 1.5°, 2°, 4°\}$, $\Omega_1 = 0$, and $\omega_1 = 77.66°$. A near circular, almost non-inclined orbit placed in Geosynchronous radii was set as the target orbit, O_2, where $a_2 = r_{GEO}$, $e_2 = 0.001$, $i_2 = 0.1°$, $\Omega_2 = \Omega_1$, and $\omega_2 = \omega_1$.

Figure 4 shows the ΔV as a function of the apogee difference, $(r_{GEO} - Q)$. The colour denotes the inclination of the O_1. In general, the required ΔV to reach a geosynchronous orbit is less than $50\ m/s$ when $i_1 \leq 0.5°$. On the other hand, when $i_1 \geq 2°$, the required ΔV is higher than $100\ m/s$, which indicates high cost for such kind of manoeuvres. If we set eq. 3 as $(r_{GEO} - Q) = 530 \cdot C_r \frac{A}{m} + 220$, then the vertical grey and black lines of fig.4 correspond to the apogee difference for $C_r = 1.3$ and $A/m = 0.0128\ m^2/kg$ and $A/m = 0.2\ m^2/kg$ (mean and max value for Payloads according to DISCOS's data), respectively. In order to minimize the cost of the manoeuvre, the orbits in sub-GEO and the GEO protected region should not differ in inclination more than $0.5°$.

3.4. Eccentricity growth and re-entry options

In this study, we focused on the low eccentricity and low inclination sub-GEO region, where eccentricity remains bounded. Recently, a full cartography study of the circumterrestrial phase space, covering altitudes from LEO-to-GEO and beyond, as also a wide range of eccentricities (up to 0.9) and inclinations (up to 120°), have been performed by Rosengren et al., 2019 [11], and a detailed study on the dynamics of the extended Geosynchronous orbital regions, including also the sub- and super- GEO regions, have been performed by Gkolias and Colombo, 2019 [7]. In these studies, it is shown that for inclinations below $\sim 40°$, there is a natural deficiency of eccentricity growth orbits, and the search for stable solution is the only option as a design plan. For inclinations above $\sim 40°$, plenty re-entry orbits exist. For these orbits, the third-body perturbations are prevailing over the other perturbations leading to large eccentricity variations for inclined orbits.

[5]The software (pykep) has been developed by ESA's pagmo development team and is free available at https://esa.github.io/pykep/index.html

4. CONCLUSIONS AND FUTURE WORK

In this study, the sub-GEO region has been examined with focus on low-to-moderate inclinations and eccentricity values. According to the results, the compliant apogee difference, for at least 100yr, is minimising when the apsidal line of the orbit is Sun-pointing, and is up to $\sim$ 250 km for low initial inclination values, and up to $\sim$ 600 km for moderate initial eccentricities (up to 0.2) and inclination (up to $\sim 18°$) values. When a wide range of Area-to-mass ratio values is examined, the compliant apogee difference found to depend on A/m value, and not on C_r, though the equation $(r_{GEO} - Q) = b_r \cdot C_r \cdot \frac{A}{m} + c$, with $b_r \sim 530\ km \cdot kg \cdot m^{-2}$ and $c \sim 220\ km$, when $e \leq 0.01$ and a non Sun-pointing orientation is considered.

Finally, the ΔV required to transfer from the sub-GEO region to an near-circular and non-inclined orbit GEO orbit was examined. According to the results, low-cost manoeuvrers with $\Delta V < 50\ m/s$ could be achieved if the difference in inclination of the starting and the target orbits is less than $0.5°$.

In order to validate the apogee difference limit shown here, a more general and stochastic analysis needed to

be performed, where other parameters should also be examined, like dependence on epoch, position with respect to the Moon and Sun etc.

ACKNOWLEDGMENTS

The authors would like to acknowledge Ioannis Gkolias for the fruitful discussions during the early phases of the project. Special thanks go to Vitali Braun for useful discussions on the ESA DRAMA suite, to Silvia Sanvido for the technical support on OSCAR, and Frazer McLean for the technical support on DISCOS.

REFERENCES

1. Anselmo A., Pardini C., (2008). Space debris mitigation in geosynchronous orbit, *Advance in Space Research*, **41**, 1091–1099
2. Braun V., Sánchez-Ortiz N., Gelhaus J., Kebschull C., Flegel S., Moeckel M., Wiedemann C., Krag H., Vörsmann P., (2013). Upgrade of the ESA DRAMA OSCAR tool: Analysis of disposal strategies considering current standards for future solar and geomagnetic activity, *In: 6th European Conference on Space Debris*, Darmstadt, Germany, 22-25 April 2013, published by the ESA
3. Chao C.-C., Campbell, S. (2005). Long-Term Perigee Height Variations of Geo Disposal Orbits a Revisit, *In: 4th European Conference on Space Debris*, Darmstadt, Germany, 18-20 April 2005, published by ESA
4. Delong N., Fremeaux C., (2005). Eccentricity management for Geostationary satellites during end of life operations, *In: 4th European Conference on Space Debris*, Darmstadt, Germany, 18-20 April 2005, published by ESA
5. ESA Space Debris Office (2021). Classification of geosynchronous objects. issue 23, *GEN-DB-LOG-00290-OPS-SD*, ESA/ESOC, Darmstadt, Germany.
6. ESA (2015). ESA space debris mitigation compliance verifications guidelines, *ESSB-HB-U-002*.
7. Gkolias I, Colombo C., (2019). Towards a sustainable exploitation of the geosynchronous orbital region, *Celestial Mechanics and Dynamical Astronomy*, **131**, 19
8. IADC (2011). IADC space debris mitigation guidelines, http://www.iadc-online.org/
9. Lewis H.G., Swinerd G.G., Martin C.E., Campbell W.S., (2004) The stability of the disposal orbits at super-synchronous altitudes, *Acta Astronautica*, **55**, 299–310
10. McLean F., Lemmens S., Funke Q., Braun V., (2017). DISCOS 3: An improved data model for ESA's Database and Information System Characterising Objects in Space, *In: 7th European Conference on Space Debris*, Darmstadt, Germany, 17-21 April 2017, published by ESA Space Debris Office.
11. Rosengren A. J., Skoulidou D. K. Tsiganis, K., Voyatzis, G., (2019). Dynamical cartography of Earth satellite orbits, *Advance in Space Research*, **63**, 443-460
12. Vallado, D. A. (2013). Fundamentals of Astrodynamics and Applications. Microcosm Press, Hawthorne, CA, 4 edition.